

## ARTICLES

## Molecular Dynamics and NMR Spin Relaxation in Proteins

DAVID A. CASE

*Department of Molecular Biology, The Scripps Research Institute, La Jolla, California 92037*

## ABSTRACT

Molecular dynamics simulations often play a central role in the analysis of biomolecular NMR data. The focus here is on NMR spin-relaxation, which can provide unique insights into the time-dependence of conformational fluctuations, especially on picosecond to nanosecond time scales which can be directly probed by simulations. A great deal has been learned from such simulations about the general nature of such motions and their impact on NMR observables. In principle, relaxation measurements should also provide valuable benchmarks for judging the quantitative accuracy of simulations, but there are a variety of experimental and computational obstacles to making useful direct comparisons. It seems likely that simulations on time scales that are just now becoming generally feasible may provide important new information on internal motions, overall rotational diffusion, and the coupling between internal and rotational motion. Such information could provide a sound foundation for a new generation of detailed interpretation of NMR spin-relaxation results.

## Introduction

Molecular dynamics (MD) simulations of proteins are now about 25 years old.<sup>1</sup> They have become increasingly common and useful as force fields have improved (providing more realistic descriptions of microscopic forces) and as computers have become more powerful (allowing longer simulations that explore more of the available conformational space). It was clear from quite early times that simulations could be useful in interpreting NMR experiments, both for fast motions seen primarily in NMR relaxation<sup>2,3</sup> and for the much slower motions relevant to “chemical exchange”. Subsequent development of sophisticated experimental methods for following spin relaxation, particularly in isotopically labeled samples, has led to renewed interest in exploring dynamical connections between simulation and experiment.

Although there are many ways in which simulations illuminate NMR experiments, I will limit the discussion here to the consideration of picosecond and nanosecond motions as monitored by NMR relaxation. Microscopic

MD simulations can be used to suggest models (generally with adjustable parameters) that capture the important characteristics expected of biomolecular motion. Experimental data is then interpreted with the aid of these models, adjusting parameters and examining the quality of the resulting fits. There exists a long-standing hope that results of such comparisons might be “turned around” to point to specific deficiencies in simulations and thus lead to better force fields or simulation procedures. The next sections discuss progress and obstacles in these areas, summarizing some of what we know from MD simulations and what we might expect soon. Many of these subjects have recently been reviewed at greater length elsewhere.<sup>4–7</sup>

## Brief Overview of NMR Relaxation Theory

In kinetics, “relaxation” refers to the time course of the return of a system to equilibrium following a small perturbation. NMR relaxation is qualitatively different from more conventional experiments (such as temperature or pH-jump experiments) in that the nuclear spin degrees of freedom (which are perturbed) involve extremely small energies and are only very weakly coupled to the ordinary conformational dynamics of the molecule. This has two important consequences. First, the ordinary chemical energies and dynamical properties of the system are almost completely unaffected by spin-flips that arise from NMR pulses, so that (from a chemical point of view) the system remains at equilibrium throughout the experiment. Second, because of the weak coupling between spin variables and molecular motion, fast atomic motions (on the picosecond and nanosecond time scales) manifest themselves in much slower relaxation of the spins (generally on the millisecond to second time scales) that can be readily studied. The presence of NMR probes throughout the molecule thus provides a unique opportunity to study the details of dynamical fluctuations.

The fundamentals of NMR relaxation theory have been presented in many places,<sup>5,6,8</sup> and there is no space here to give more than a taste of what is involved. The rate of return of a spin system to equilibrium is determined by the time-dependent magnetic fields experienced at each atomic nucleus, arising from molecular motions. The ability of this stochastic, fluctuating field to induce spin transitions is dependent upon its intensity at frequencies that correspond to sums and differences of the Larmor frequencies of the nuclear spins. These are represented as “spectral densities”  $J(\omega)$ , which in turn are the Fourier transforms of microscopic time-correlation functions. For example, the ability of an amide proton to relax the spin of the <sup>15</sup>N nucleus to which it is attached can be expressed in terms of the time-correlation function

$$C(\tau) \equiv \langle P_2[\boldsymbol{\mu}(t) \cdot \boldsymbol{\mu}(t + \tau)] \rangle \quad (1)$$

David Case received a B.S. degree from Michigan State (working with Tom Pinnavaia and Jim Harrison) and a Ph.D. from Harvard (working with Dudley Herschbach and Martin Karplus). He was on the faculty of the University of California, Davis, for nine years before moving to his present position at The Scripps Research Institute in 1986. His research efforts are in the area of theoretical and computational chemistry, with emphases on computational aspects of biomolecular NMR, electronic structures of active sites of metalloproteins, and molecular dynamics simulations of proteins and nucleic acids.

where  $\mu(t)$  is the (time-dependent) unit vector from the nitrogen to the proton,  $P_2(\cos \theta) \equiv (3 \cos^2 \theta - 1)/2$  is a Legendre polynomial, and the brackets indicate a time and ensemble average over all conformations of the system. The spectral density  $J(\omega)$  is then the Fourier transform of  $C(\tau)$ . To be effective in relaxation,  $J(\omega)$  needs to be large near the Larmor frequency of the spins or near zero frequency. As it happens, the most important molecular motion for biomolecules (from the standpoint of NMR spin relaxation) is overall rotational diffusion or tumbling. It is this fact that makes NMR structure determination possible in the first place: to a good first approximation, proton relaxation (as monitored by nuclear Overhauser effect measurements) can be interpreted as arising from the rotational Brownian motion of a *rigid* molecule, and the atomic coordinates of this hypothetical rigid structure can be adjusted to optimize agreement with the NMR data. It is important to note that this does not mean that internal deformations are not present, but only that most such motions are fairly inefficient in driving NMR spin relaxation. In general, a more careful quantitative analysis (usually involving measurements of “heteronuclear”  $^{13}\text{C}$  or  $^{15}\text{N}$  relaxation) is required to extract information about internal motions from NMR data.

## Rotational Diffusion

These considerations point to the importance of biomolecular NMR for understanding rotational diffusion, including not only the overall tumbling times but also the anisotropy of this motion (since nonspherical molecules will tumble more rapidly about some directions than others). Molecular dynamics simulations are now able to explore directly the nanosecond time scales of biomolecular rotational diffusion, but most theories of this behavior are still based on diffusion models. These postulate that the probability density  $f(\Phi, t)$  of having a molecule with orientation  $\Phi$  at time  $t$  is governed by a diffusion equation, which for a spherical molecule is

$$\frac{\partial}{\partial t} f(\Phi, t) = D \nabla^2 f(\Phi, t) \quad (2)$$

The Stokes–Einstein–Debye relation gives  $D = kT/(8\pi R_h^3 \eta)$ , where  $\eta$  is the macroscopic solvent viscosity and  $R_h$  is the hydrodynamic radius of the macromolecule. For a rigid molecule undergoing such isotropic Brownian rotational motion, the  $P_2$  time-correlation functions for all internuclear vectors are the same: an exponential  $C(\tau) = \exp(-\tau/\tau_c)$ , where the time constant  $\tau_c$  is  $1/6D$ . Its Fourier transform is then a Lorentzian:

$$J^{\text{rigid}}(\omega) = \frac{2\tau_c}{1 + \omega^2\tau_c^2} \quad (3)$$

**Measuring Rotational Diffusion Constants.** Any single relaxation parameter (such as  $T_1$ ,  $T_2$ ,  $T_{1\rho}$ , or NOE) is determined by a combination of spectral densities and molecular structure (which determines interatomic distances, and hence the strength of the dipole–dipole

interactions that dominate most spin relaxation). Sometimes, however, ratios of relaxation parameters become independent (or nearly so) of the structure, and this allows one to estimate rotational parameters more directly from NMR data. The most celebrated and useful of these relations is the ratio of longitudinal to transverse relaxation rates: for a very simplified model in which the mean square field is the same in all directions,<sup>9</sup>

$$T_1/T_2 = 1 + \omega^2\tau_c^2/2 \quad (4)$$

Actual analyses of NMR relaxation data use more complex equations that model the physical origins of the fluctuating fields, but it can be difficult to ensure that everything has been properly accounted for. The following paragraphs outline some of difficulties that arise.

1. Most biomolecules tumble in an anisotropic fashion, so that some interatomic vectors rotate faster than others. In favorable cases, where data can be extracted from a large number of vectors whose directions are roughly uniformly distributed, an estimate of the anisotropy of rotation can be made even in the absence of a structural model.<sup>10</sup> More generally, however, some structural information is needed, so that angles between internuclear vectors and the principal axes of rotational diffusion can be determined.<sup>11–13</sup> This analysis is complicated by the potential presence of internal motions that can have similar time scales, and which themselves may also be anisotropic. For example, some early applications of the model-free analysis (discussed below) failed to fully appreciate the complications arising from even fairly small anisotropies in rotational tumbling, leading to overestimates of chemical exchange as fitting parameters took up the “slack” for an incorrect rotational model. This potential problem is now much better understood,<sup>13,14</sup> but it is still possible that incorrect assumptions about the nature or extent of internal motions could lead to uncertainties in parameters describing the overall rotational motion.

2. There is also concern that relaxation pathways other than dipolar coupling (particularly from sample heterogeneity or slow conformational transitions) will affect  $T_2$  in ways that are systematically different than  $T_1$ . For example, Lee and Wand have shown that  $\tau_c$  values determined at multiple field strengths for ubiquitin (which is fairly isotropic) are about 15% higher if experimental  $T_2$  values are included in the data fitting scheme, compared to fits that rely only on  $T_1$  and NOE measurements.<sup>15</sup> Also, analyses of proton relaxation data seem to give significantly shorter rotational correlation times than do fits based on carbon or nitrogen data.<sup>16</sup> Some recent suggestions about how to distinguish chemical exchange from anisotropic diffusion in  $T_2$  measurements may help to make this sort of data analysis more consistent.<sup>13,14</sup>

3. It can be difficult to interpret results when experiments are carried out under different conditions of viscosity and temperature. An approximate correction to standard conditions can be made by assuming that the rotational diffusion constants follow the Stokes–Einstein–Debye relationship, such that  $D$  is proportional to  $\eta/T$ . It

is then straightforward to correct most measurements in dilute solutions to standard conditions (e.g., 20 °C in H<sub>2</sub>O) using the known temperature-dependent viscosity of H<sub>2</sub>O or D<sub>2</sub>O, although in practice this is not often reported. Because the sensitivity of the NMR experiment is low, samples are often fairly concentrated and may have some amount of aggregation present as well, both of which can complicate the interpretation of fitted diffusion constants.<sup>17,18</sup>

Under these circumstances, it would clearly be desirable to have independent means of assessing rotational tumbling times. Other experimental techniques applicable to biomolecules include analysis of depolarized dynamic light scattering<sup>19</sup> and the decay of fluorescence anisotropy. In many cases (but not all<sup>20</sup>), tumbling times derived from fluorescence anisotropy measurements are shorter than those derived from NMR, and the differences are sometimes dramatic.<sup>21–24</sup> In at least some of these cases, the NMR results follow the expected  $\eta/T$  dependence on temperature and viscosity,<sup>24</sup> and fluorescence measurements show no evidence of concentration-dependent effects (W. J. Chazin, personal communication). The origins of these discrepancies are still not well understood. Light scattering measurements, on the other hand, appear to give results more in line with those extracted from NMR.<sup>19</sup>

**Computational Approaches.** For proteins of known structure, hydrodynamic “bead” models can be constructed that allow one to estimate rotational diffusion constants.<sup>25</sup> These calculations, however, require assumptions about what boundary conditions for the diffusion equations are most appropriate,<sup>6</sup> along with an understanding of how waters of hydration affect molecular tumbling. The latter are usually modeled by including a shell of waters at the molecular surface as part of the macromolecule, with the thickness of this shell being treated as an empirical parameter. In a recent study, shells of water between 2.3 and 4.3 Å were found to give good agreement with rotational diffusion constants extracted from NMR relaxation measurements.<sup>25</sup> Such calculations are thus helpful in ruling out fits to NMR data with unphysical parameters, but otherwise have a fairly large uncertainty: the diffusion constant calculated for lysozyme with a water shell of 2 Å is 40% greater than that predicted for a shell of 4 Å.

What might molecular dynamics simulations be able to contribute to this situation? Although few simulations even today are long enough to give a good statistical description of molecular rotation, it has been recognized for some time that a rough account of molecular tumbling can be gained from time-correlation functions even at fairly short times.<sup>26</sup> Figures 1 and 2 illustrate some results from a recent 8 ns simulation of *Escherichia coli* thioredoxin. Figure 1 shows three time-correlation functions (eq 1) determined from the simulation *after* overall rotation had been removed by superposing each MD snapshot onto the average conformation; this is the usual method of analysis. The upper two N–H vectors (for phe27 and leu78) show typical behavior for relatively rigid

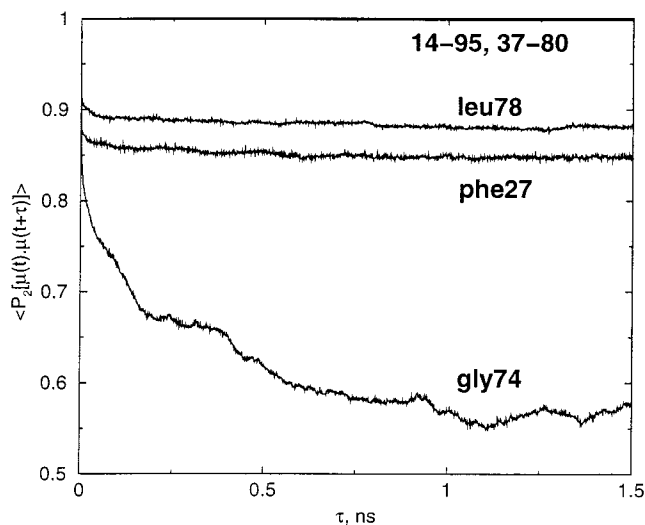


**FIGURE 1.** Time-correlation functions for thioredoxin, after removing overall rotation. Results for three N–H vectors are shown; correlations functions for the “long” axes (connecting N of residues on opposite sides of the protein) do not visibly change from unity on the scale of this figure. The correlation functions at 3 ns are essentially unchanged from those shown here at 1.5 ns.

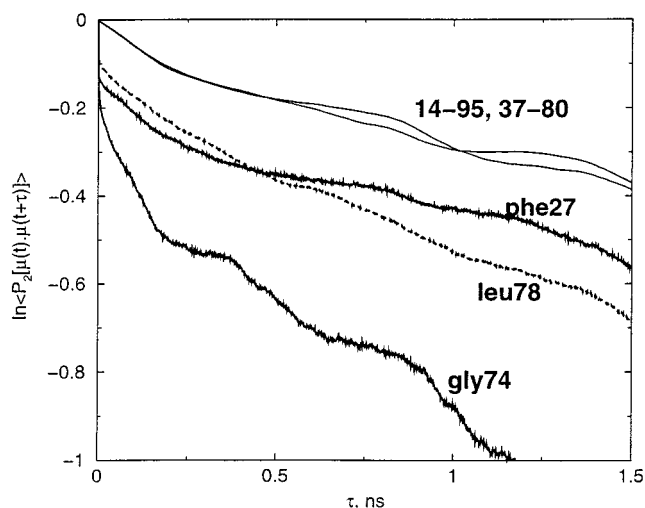


**FIGURE 2.** Time-correlation functions for thioredoxin, before removing overall rotation. Vectors are the same as in Figure 1.

parts of proteins: there is rapid (subpicosecond) decay of  $C(\tau)$  from 1.0 to around 0.9, arising from vibrational motion. This is followed by a slower decay (with an amplitude of about 0.03 and a time scale of 20–50 ps) that primarily arises from librational motion of the peptide group as a whole. Beyond about 50 ps the correlation functions are flat, even well beyond the time scale shown in the figure: the computed correlation function at 1.5 ns differs from that at 200 ps by less than 0.005. Also shown is the correlation function for a residue in a more mobile region (gly74), with an experimental  $S^2$  value of about 0.5;<sup>27</sup> this shows clear evidence for internal motions on a nanosecond time scale, but the correlation function does appear to reach a plateau value for the 1–3 ns period that is near the experimental value.

Figure 2, on the other hand, shows results for the same interatomic vectors from the “raw” simulation, including



both internal motion and overall rotational tumbling. These are plotted on a semilog scale, so that exponential decay would be represented by a straight line. The correlation function decay for the two fairly rigid N–H spin pairs over the 0.2–1 ns time range roughly parallels that of the long vectors, corresponding to the initial stages of rotational diffusion with a tumbling time of about 4.5 ns. This is in qualitative accord with NMR relaxation measurements,<sup>24,27</sup> but the statistical uncertainties become severe for such correlation functions,<sup>28</sup> so that they are useful only for times that are a small fraction of the MD simulation length. Much longer simulation times would be needed to obtain any sort of precise estimate or to identify coupling between internal modes and overall tumbling or the multiple exponential decays expected for anisotropic diffusion. Averaging over multiple vectors (as is done to extract overall tumbling times from NMR relaxation data) should improve the statistics somewhat. Having simulations an order of magnitude longer, which would cover several rotational periods, would clearly be helpful in developing a microscopic picture of rotational diffusion; a few such simulations are available today, and many more should be available soon. It remains to be seen, of course, whether current force fields, particularly for water, are accurate enough to provide good estimates for macromolecular rotational diffusion. This presumably will test the effective viscosity of the water model and the strength of protein–water interactions.<sup>26</sup>

**Making Use of the Results.** There are a variety of reasons why it is important to have a good analysis of rotational diffusion. First, these parameters provide a low-resolution representation of the size and shape of the molecule. This can be very useful in checking for artifacts such as aggregation and can also provide information about gross structural features such as domain orientations.<sup>29,31</sup> Second, analysis of other types of NMR measurements is greatly facilitated when the rotational diffusion parameters are known. For example, estimates of multiple spin (“spin-diffusion”) corrections to distances derived from proton nuclear Overhauser measurements depend in an important way on the overall rotational dynamics. Estimates of internal mobility from quantitative fits to heteronuclear relaxation (discussed in the next section) are also sensitive to the time scale of overall tumbling.

## Internal Dynamics of Individual Spin Pairs

Unlike the situation for overall rotational tumbling, where the motion is expected to be primarily diffusive, there is a large range of likely internal motions (ranging from quantum zero-point librations to “jumps” between alternate conformations), so that no single model is likely to suffice. For motions that are not coupled to overall tumbling (which are arguably of small amplitude and/or fast time scale), the details are not relevant for some types of NMR relaxation measurements. For these motions, the simplest application of the Lipari–Szabo “model-free” ansatz extends eq 3 to include the effects of rapid internal

motion in an isotropically tumbling system:<sup>32</sup>

$$J^{\text{LS}} = \frac{2S^2\tau_c}{1 + \omega^2\tau_c^2} + \frac{2(1 - S^2)\tau}{1 + \omega^2\tau^2} \quad (5)$$

Here,  $S^2$  is an order parameter describing the angular extent of internal motion, and  $\tau^{-1} = \tau_c^{-1} + \tau_e^{-1}$ , where  $\tau_e$  is an effective time constant for the internal motion.  $J^{\text{LS}}$  is the spectral density that one would expect if overall and internal motions were decoupled, and if the internal time-correlation function decayed from its initial value of 1 to a “plateau value” of  $S^2$  with a time constant  $\tau_e$  which was short compared to  $\tau_c$ . This certainly appears to be a valid assumption for many N–H groups in regions of regular secondary structure in proteins, as seen for phe27 and leu78 in Figure 1.

It is by now quite common to measure  $T_1$ ,  $T_2$ , and NOE relaxation of amide nitrogens in proteins and to analyze the results with a model-free formalism.<sup>33</sup> In principle, these analyses should provide benchmark tests for comparison with MD simulations, but several things inhibit this:

1. Many experimental relaxation measurements have both random and systematic errors that are only approximately known.<sup>7</sup> Reasonable estimates for these uncertainties propagate into estimated standard errors of fitted parameters that are often of the order of 0.05–0.1 for  $S^2$  and (in most cases) very large for  $\tau_e$ .<sup>7,34,35</sup> For systems with anisotropic overall tumbling, any errors in the assumed structures that affect relative angles between N–H vectors will be propagated into the order parameters. Differences between samples, spectrometers, and laboratories carrying out the measurements can also have an effect on the accuracy and precision of extracted parameters.<sup>36</sup>

2. Fitting the observed relaxation data to Lipari–Szabo or other models requires certain assumptions, especially concerning the effective N–H bond distance.<sup>37–39</sup> In the extreme narrowing limit (where internal motions are very fast and the second term in eq 5 can be ignored), all dipolar relaxation rates scale as  $S^2/r_{\text{NH}}^6$ . This means that the spin behavior expected for  $S^2$  of 0.85 and  $r_{\text{NH}}$  of 1.02 Å is indistinguishable from that expected for  $S^2$  of 0.95 and  $r_{\text{NH}}$  of 1.04 Å. The “correct” effective distance that should be used is itself conventional, since it depends on a decision about how to deal with zero-point vibrational motions. They might be included as a part of the fluctuations described by  $S^2$  or might be considered a separate type of motion whose effects are folded into an effective bond length.<sup>37,39</sup> This (arbitrary) decision has little effect on relative order parameters but makes comparisons of absolute values difficult; even relative order parameters become suspect if one admits a model in which the effective bond length might not be the same for all peptide groups in the protein.

3. Similar comments apply to other models for internal motion. For example, motions of the peptide plane in proteins have been analyzed in terms of a three-dimensional Gaussian angular fluctuation (3D-GAF) model.<sup>40,41</sup> Here, the internal fluctuations of each peptide group are

taken to be distributed as Gaussian functions of torsion angles about three perpendicular local vectors. A key parameter is the amplitude of fluctuations about the  $C\alpha-C\alpha$  axis. Analysis of experimental data for ubiquitin gives fluctuation amplitudes on the order of  $16^\circ$ , assuming an N-H bond length of  $1.02 \text{ \AA}$ . This is somewhat larger than values obtained from MD simulations using the CHARMM force field. However, if the effective N-H bond length is increased to  $1.04 \text{ \AA}$ , the extracted fluctuations fall to about  $9^\circ$ , in rough agreement with the MD simulations. This illustrates one of the reasons why it has proved so difficult to test force fields through quantitative comparisons between calculated and observed NMR parameters.

4. Fits to NMR relaxation data also generally require assumptions about the magnitude and orientation of the nitrogen chemical shift anisotropy (CSA) tensor, since CSA relaxation competes with dipolar relaxation, especially at higher field strengths. If the usual assumptions are wrong, or if the CSA tensors vary in a significant way from one peptide group to the next, the fitted order parameters would again become suspect.<sup>42-44</sup> Furthermore, dipolar relaxation usually only approximately fits a two-spin model,<sup>45</sup> so that additional assumptions have to be made about distances and motional parameters for interatomic vectors other than the one whose behavior is being most directly monitored.

5. Coupling between internal motions and overall tumbling is generally not taken into account in current schemes for analyzing NMR relaxation data. As discussed above, it is also difficult to extract this sort of information from MD simulations, but it is possible to set up diffusion models that include such effects.<sup>46,47</sup> Tugarinov et al.<sup>47</sup> have analyzed experimental relaxation data for ribonuclease H using a mode-coupling diffusion equation approach to model interactions between local and global motions. The resulting order parameters are often significantly lower than those obtained from a model-free analysis that neglects interactions between local and global motions.

Some of these problems can be ameliorated by making measurements at multiple magnetic fields,<sup>7,48</sup> but they do inject a note of caution into what might be seen as straightforward comparisons between simulation and experiment. One early example of such a straightforward comparison looked at  $^{13}\text{C}\alpha$  relaxation in a zinc finger domain.<sup>49</sup> Although the solvated simulations were rather short (125 ps), both experiment and simulation yielded nearly uniform and fairly high order parameters in regions of regular secondary structure, with lower values in a loop connecting secondary structural elements and much lower values at the C-terminus (see Figure 3). This sort of qualitative accord between regions predicted (from MD simulations) to have high order parameters and fitted values from NMR relaxation experiments has been found in a great many subsequent simulations.

Of course, fluctuations and order parameters extracted from MD simulations themselves have significant random and systematic errors.<sup>28</sup> Fluctuations within a local conformational basin converge quite quickly, but dihedral

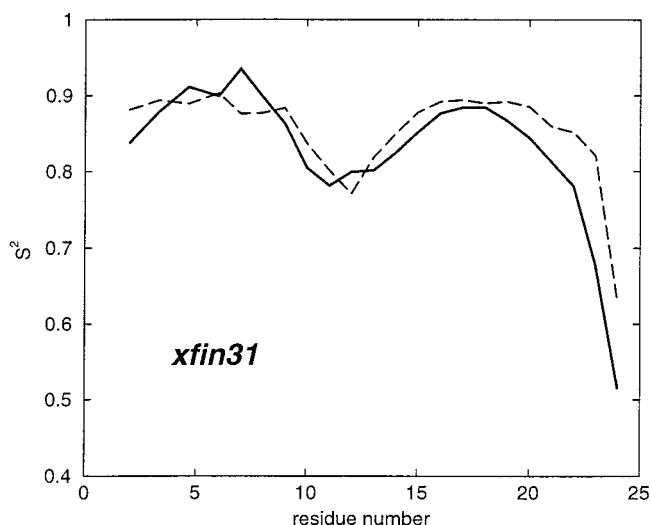


**FIGURE 3.** Simulated and measured order parameters for  $^{13}\text{C}\alpha$  relaxation in a zinc-finger peptide. Solid line from fits to NMR relaxation data, dashed line from MD simulation. Both curves have been data averaged over three-residue windows. As expected, the order parameters are highest for residues 3–9 (forming a  $\beta$ -hairpin loop) and 15–21 (which are helical). Residues at the C-terminal end of the peptide, and in the region between secondary structures, are more mobile. Data taken from ref 71.

angle transitions are often poorly sampled. This lack of adequate sampling should be especially important for small order parameters ( $S^2 < 0.6$ ) and is probably present even in the longest (and therefore most recent) simulations. The approach of simulated order parameters to their converged values need not be a monotonic function of sampling times: partial sampling of dihedral transitions can lead to time-correlation functions that are either larger or smaller than their true (converged) values.<sup>28</sup> Classical MD simulations also ignore quantum zero-point vibrations, which are expected to affect order parameters by amounts up to 0.1.<sup>50,51</sup> This is most relevant for quantitative comparisons between calculated and experimentally fitted order parameters in relatively rigid parts of proteins;<sup>39</sup> it may be most relevant to compare MD simulations to experimental order parameters that were calculated assuming an effective bond length that includes zero-point motion, as discussed in point 2, above.

Hence, for both experimental and computational reasons, early hopes that quantitative comparisons between predicted and fitted motional parameters would consistently look as favorable as those in Figure 3 have not been realized. Perhaps more typical of recent calculations are simulations on lysozyme,<sup>52,53</sup> dihydrofolate reductase,<sup>54</sup> and the  $\beta$ ARK1 PH domain.<sup>55</sup> All of these show good agreement between simulation and experiment concerning which N-H vectors have more mobility (lower order parameters) than the average found for regular regions of secondary structure. However, the simulated order parameters for the mobile regions are in many cases significantly lower than those extracted from NMR relaxation data. Other recent simulations, e.g., on ribonuclease H,<sup>36</sup> staphylococcal nuclease,<sup>45</sup> and barstar,<sup>56</sup> show similar qualitative behavior, although with fewer pronounced

deviations between simulation and experiment. It is possible that inadequate sampling of dihedral angle transitions could lead to significant overestimates of the amount of backbone motion. It is worth noting, however, that this qualitative discrepancy between simulation and NMR fits has not changed much as typical simulation times have progressed (over the past five years) from under 1 ns to nearly 10 ns, and that studies of the convergence of time-correlation functions (by breaking longer simulations into shorter pieces) generally show little evidence that longer simulations would produce significantly higher order parameters. Hence, one must also entertain the idea that current force fields allow too much motion, particularly in regions outside of regular secondary structure.

## Internal Dynamics of Multiple Spins

The previous section dealt with the dynamical behavior of individual interatomic vectors. It is clearly of interest to work toward a consistent account of correlated dynamics as well. In addition to its intrinsic interest, such an account could have important practical consequences for structure determination. For example, measurement of order parameters for N–H or C–H vectors gives no direct information about the effects of internal motion on the H–H vectors that are the primary input to NMR structure refinements. The development of models that go beyond single spin pairs could allow information gained from  $^{13}\text{C}$  or  $^{15}\text{N}$  measurements to be transferred into the proton realm.<sup>57,58</sup>

There are two basic ways this sort of information can currently be extracted from NMR measurements. First, relaxation measurements can be made for more than one interatomic vector in fairly rigid groups, such as the peptide planes of proteins.<sup>5,40</sup> These data can be used to check the consistency of various NMR measurements and to probe the anisotropy of internal motion. Second, one can carry out “cross-correlated” relaxation measurements that explicitly depend on the properties of more than one interatomic vector at a time.<sup>5</sup> Both of these approaches are in a state of rapid development on the NMR side and should provide a great deal of useful information in the coming years.

## Conclusions

In this Account, I have had space to deal with only one aspect of the connections between biomolecular NMR and molecular dynamics simulations, concentrating on NMR relaxation in the backbones of proteins. This is probably the most active area of investigation, but similar considerations arise in studies of dynamical motions in protein side chains or in nucleic acids. As outlined above, there are legitimate reasons to be cautious when examining comparisons between NMR relaxation measurements and molecular dynamics simulations. On the NMR side, measurements at multiple magnetic fields often help enormously in validating the relaxation analysis and in increasing the ratio of measurements to adjustable

parameters. Measurements of the properties of additional interatomic vectors (such as C'–N, C'–C $\alpha$ , or C'–H) or of cross-correlated relaxation have much the same beneficial effect.

On the computational side, the most promising near-term advance may simply be to carry out longer simulations on a more routine basis, since there seems to be no other simple way to address the questions of convergence. As an example of what may be possible, consider the internal fluctuations of the gly74 N–H vector shown in Figure 1. In an 8 ns simulation, this correlation function does appear to reach a plateau value (which happens here to be in good agreement with the order parameters extracted from experiment); in shorter simulations, such a vector would just seem to be unconverged and uninterpretable in a quantitative sense. It is likely that simulations yet 10 times longer still would show a broader range of internal motions that were usefully sampled, along with fundamentally new ideas about rotational diffusion and about the possible couplings between internal and rotational motion. In view of the significant effects that have been predicted for the coupling between internal and overall motion based on mode-coupling models,<sup>47</sup> even qualitative information at these longer time scales may be most helpful. Overall, the interplay between NMR relaxation and MD simulations should continue to be fascinating and informative for many years.

*This work was supported by NIH Grant GM45811. I thank Walter Chazin for providing results of unpublished studies on calbindin.*

## References

- (1) McCammon, J. A.; Gelin, B. R.; Karplus, M. Dynamics of folded proteins. *Nature* **1977**, *267*, 585–590.
- (2) Levy, R. M.; Karplus, M.; Wolynes, P. G. NMR relaxation parameters with internal motion: Exact Langevin trajectory results compared with simplified relaxation models. *J. Am. Chem. Soc.* **1981**, *103*, 5998–6011.
- (3) Lipari, G.; Szabo, A.; Levy, R. M. Protein dynamics and NMR relaxation: comparison of simulations with experiment. *Nature* **1982**, *300*, 197–198.
- (4) Daragan, V. A.; Mayo, K. H. Motional model analyses of protein and peptide dynamics using  $^{13}\text{C}$  and  $^{15}\text{N}$  NMR relaxation. *Prog. Nucl. Magn. Reson. Spectrosc.* **1997**, *31*, 63–105.
- (5) Fischer, M. W. F.; Majumdar, A.; Züderweg, E. R. P. Protein NMR relaxation: theory, applications and outlook. *Prog. Nucl. Magn. Reson. Spectrosc.* **1998**, *33*, 207–272.
- (6) Korzhnev, D. M.; Billeter, M.; Arseniev, A. S.; Orekhov, V. Y. NMR studies of tumbling and internal motions in proteins. *Prog. Nucl. Magn. Reson. Spectrosc.* **2001**, *38*, 197–266.
- (7) Palmer, A. G., III. NMR probes of molecular dynamics: overview and comparison with other techniques. *Annu. Rev. Biophys. Biomol. Struct.* **2001**, *30*, 129–155.
- (8) Goldman, M. *Quantum Description of High-Resolution NMR in Liquids*; Clarendon Press: Oxford, 1988.
- (9) van de Ven, F. J. M. *Multidimensional NMR in Liquids. Basic Principles and Experimental Methods*; Wiley-VCH: New York, 1995.
- (10) Clore, G. M.; Gronenborn, A. M.; Szabo, A.; Tjandra, N. Determining the magnitude of the fully asymmetric diffusion tensor from heteronuclear relaxation data in the absence of structural information. *J. Am. Chem. Soc.* **1998**, *120*, 4889–4890.
- (11) Andrec, M.; Inman, K. G.; Montelione, G. T. A Bayesian statistical method for the detection and quantification of rotational diffusion anisotropy from NMR relaxation data. *J. Magn. Reson.* **2000**, *146*, 66–80.
- (12) Blackledge, M.; Cordier, F.; Marion, D. Precision and uncertainty in the characterization of anisotropic rotational diffusion by  $^{15}\text{N}$  relaxation. *J. Am. Chem. Soc.* **1998**, *120*, 4538–4539.



- (13) Kroenke, C. D.; Loria, J. P.; Lee, L. K.; Rance, M.; Palmer, A. G., III. Longitudinal and transverse  $^1\text{H}$ - $^{15}\text{N}$  dipolar/ $^{15}\text{N}$  chemical shift anisotropy relaxation interference: Unambiguous determination of rotational diffusion tensors and chemical exchange effects in biological macromolecules. *J. Am. Chem. Soc.* **1998**, *120*, 7905–7915.
- (14) Pawley, N. H.; Wang, C.; Koide, S.; Nicholson, L. K. An improved method for distinguishing between anisotropic tumbling and chemical exchange in analysis of  $^{15}\text{N}$  relaxation parameters. *J. Biomol. NMR* **2001**, *20*, 149–165.
- (15) Lee, A. L.; Wand, A. J. Assessing potential bias in the determination of rotational correlation times of proteins by NMR relaxation. *J. Biomol. NMR* **1999**, *13*, 101–112.
- (16) Tonelli, M.; Ragg, E.; James, T. L. Nuclear magnetic resonance structure of d(GCATATGATAG).d(CTATCATATGC): A consensus sequence for promoters recognized by OK RNA polymerase. *Biochemistry* **1998**, *37*, 11745–11761.
- (17) Schurr, J. M.; Babcock, H. P.; Fujimoto, B. S. A test of model-free formulas. Effects of anisotropic rotational diffusion and dimerization. *J. Magn. Reson. Ser. B* **1994**, *105*, 211–224.
- (18) Fushman, D.; Cahill, S.; Cowburn, D. The main-chain dynamics of the dynamin pleckstrin homology (PH) domain in solution: Analysis of  $^{15}\text{N}$  relaxation with monomer/dimer equilibration. *J. Mol. Biol.* **1997**, *266*, 173–194.
- (19) Eimer, W.; Williamson, J. R.; Boxer, S. G.; Pecora, R. Characterization of the overall and internal dynamics of short oligonucleotides by depolarized dynamic light scattering and NMR relaxation measurements. *Biochemistry* **1990**, *29*, 799–811.
- (20) Moncrieffe, M. C.; Jaranic, N.; Kemple, M. D.; Potter, J. D.; Macura, S.; Predergast, F. G. Structure-fluorescence correlations in a single tryptophan mutant of carp parvalbumin: Solution structure, backbone and side-chain dynamics. *J. Mol. Biol.* **2000**, *297*, 147–163.
- (21) Nordlund, T. M.; Andersson, S.; Nilsson, L.; Rigler, R.; Graslund, A.; McLaughlin, L. W. Structure and dynamics of a fluorescent DNA oligomer containing the EcoRI recognition sequence: Fluorescence, molecular dynamics and NMR studies. *Biochemistry* **1989**, *28*, 9095–9103.
- (22) Guest, C. R.; Hochstrasser, R. A.; Sowers, L. C.; Millar, D. P. Dynamics of mismatched base pairs in DNA. *Biochemistry* **1991**, *30*, 3271–3279.
- (23) Palmer, A. G., III; Hochstrasser, R. A.; Millar, D. P.; Rance, M.; Wright, P. E. Characterization of amino acid side chain dynamics in a zinc-finger peptide using  $^{13}\text{C}$  NMR spectroscopy and time-resolved fluorescence spectroscopy. *J. Am. Chem. Soc.* **1993**, *115*, 6333–6345.
- (24) Kemple, M. D.; Yuan, P.; Nollet, K. E.; Fuchs, J. A.; Silva, N.; Predergast, F. G.  $^{13}\text{C}$  NMR and fluorescence analysis of tryptophan dynamics in wild-type and two single-trp variants of *Escherichia coli* thioredoxin. *Biophys. J.* **1994**, *66*, 2111–2126.
- (25) García de la Torre, J.; Huertas, M.; Carrasco, B. HydroNMR: Prediction of NMR relaxation of globular proteins from atomic-level structures and hydrodynamic calculations. *J. Magn. Reson.* **2000**, *147*, 138–146.
- (26) Smith, P. E.; van Gunsteren, W. F. Translational and rotational diffusion of proteins. *J. Mol. Biol.* **1994**, *236*, 629–636.
- (27) Stone, M. J.; Chandrasekhar, K.; Holmgren, A.; Wright, P. E.; Dyson, H. J. Comparison of backbone and tryptophan side-chain dynamics of reduced and oxidized *Escherichia coli* thioredoxin using  $^{15}\text{N}$  NMR relaxation measurements. *Biochemistry* **1993**, *32*, 426–435.
- (28) Frenkel, D.; Smit, B. *Understanding Molecular Simulation: From Algorithms to Applications*; Academic Press: San Diego, 1996.
- (29) Brüschweiler, R.; Liao, X.; Wright, P. E. Long-range motional restrictions in a multidomain zinc-finger protein from anisotropic tumbling. *Science* **1995**, *268*, 886–889.
- (30) Hus, J.-C.; Marion, D.; Blackledge, M. De novo determination of protein structure by NMR using orientational and long-range order restraints. *J. Mol. Biol.* **2000**, *298*, 927–936.
- (31) Ghose, R.; Fushman, D.; Cowburn, D. Determination of rotational diffusion tensor of macromolecules in solution from NMR relaxation data with a combination of exact and approximate methods. Application to the determination of interdomain orientation in multidomain proteins. *J. Magn. Reson.* **2001**, *149*, 204–217.
- (32) Lipari, G.; Szabo, A. Model-free approach to the interpretation of nuclear magnetic resonance relaxation in macromolecules. I. Theory and range of validity. *J. Am. Chem. Soc.* **1982**, *104*, 4546–4559.
- (33) Goodman, J.; Pagel, M.; Stone, M. Relationships between protein structure and dynamics from a database of NMR-derived backbone order parameters. *J. Mol. Biol.* **2000**, *295*, 963–978.
- (34) Andrec, M.; Montelione, G. T.; Levy, R. M. Estimation of dynamic parameters from NMR relaxation data using the Lipari-Szabo model-free approach and Bayesian statistical methods. *J. Magn. Reson.* **1999**, *139*, 408–421.
- (35) Daragan, V. A.; Mayo, K. H. Using the model free approach to analyze NMR relaxation data in cases of anisotropic molecular diffusion. *J. Phys. Chem. B* **1999**, *103*, 6829.
- (36) Philippopoulos, M.; Mandel, A. M.; Palmer, A. G., III; Lim, C. Accuracy and precision of NMR relaxation experiments and md simulations for characterizing protein dynamics. *Proteins* **1997**, *28*, 481–493.
- (37) Henry, E. R.; Szabo, A. Influence of vibrational motion on solid-state line shapes and NMR relaxation. *J. Chem. Phys.* **1985**, *82*, 4753–4761.
- (38) Ottiger, M.; Bax, A. Determination of relative N–HN, N–C', and C $\alpha$ –H $\alpha$  effective bond lengths in a protein by NMR in a dilute liquid crystalline phase. *J. Am. Chem. Soc.* **1998**, *120*, 12334–12341.
- (39) Case, D. A. Calculations of NMR dipolar coupling strengths in model peptides. *J. Biomol. NMR* **1999**, *15*, 95–102.
- (40) Bremi, T.; Brüschweiler, R. Locally anisotropic internal polypeptide backbone dynamics by NMR relaxation. *J. Am. Chem. Soc.* **1997**, *119*, 6672–6673.
- (41) Lienin, S. F. Anisotropic Dynamics in Molecular Systems Studied by NMR Relaxation. Ph.D. Thesis, ETH-Zürich, 1998.
- (42) Fushman, D.; Tjandra, N.; Cowburn, D. Direct measurement of  $^{15}\text{N}$  chemical shift anisotropy in solution. *J. Am. Chem. Soc.* **1998**, *120*, 10947–10952.
- (43) Kroenke, C. D.; Rance, M.; Palmer, A. G., III. Variability of the  $^{15}\text{N}$  chemical shift anisotropy in *Escherichia coli* ribonuclease H in solution. *J. Am. Chem. Soc.* **1999**, *121*, 10119–10125.
- (44) Renner, C.; Holak, T. A. Separation of anisotropy and exchange broadening using  $^{15}\text{N}$  CSA- $^{15}\text{N}$ - $^1\text{H}$  dipole-dipole relaxation cross-correlation experiments. *J. Magn. Reson.* **2000**, *145*, 192–200.
- (45) Chatfield, D. C.; Szabo, A.; Brooks, B. R. Molecular dynamics of staphylococcal nuclease: Comparison of simulation with  $^{15}\text{N}$  and  $^{13}\text{C}$  relaxation data. *J. Am. Chem. Soc.* **1998**, *120*, 5301–5311.
- (46) Fausti, S.; La Penna, G.; Cuniberti, C.; Perico, A. Mode-coupling Smoluchowski dynamics of a double-stranded DNA oligomer. *Biopolymers* **1999**, *50*, 613–629.
- (47) Tugarinov, V.; Liang, Z.; Shapiro, Y. E.; Freed, J. H.; Meirovitch, E. A structural mode-coupling approach to  $^{15}\text{N}$  relaxation in proteins. *J. Am. Chem. Soc.* **2001**, *123*, 355–3063.
- (48) Fushman, D.; Tjandra, N.; Cowburn, D. An approach to direct determination of protein dynamics from  $^{15}\text{N}$  NMR relaxation at multiple fields, independent of variable  $^{15}\text{N}$  chemical shift anisotropy and chemical exchange contributions. *J. Am. Chem. Soc.* **1999**, *121*, 8577–8582.
- (49) Palmer, A. G.; Case, D. A. Molecular dynamics analysis of NMR relaxation in a zinc-finger peptide. *J. Am. Chem. Soc.* **1992**, *114*, 9059–9067.
- (50) Brüschweiler, R. Normal modes and NMR order parameters in proteins. *J. Am. Chem. Soc.* **1992**, *114*, 5341–5344.
- (51) Brüschweiler, R.; Case, D. A. Characterization of biomolecular structure and dynamics by NMR cross-relaxation. *Prog. Nucl. Magn. Reson. Spectrosc.* **1994**, *26*, 27–58.
- (52) Smith, L. J.; Mark, A. E.; Dobson, C. M.; van Gunsteren, W. F. Comparison of md simulations and NMR experiments for hen lysozyme. analysis of local fluctuations, cooperative motions, and global changes. *Biochemistry* **1995**, *34*, 10918–10931.
- (53) Stocker, U.; van Gunsteren, W. F. Molecular dynamics simulation of hen egg white lysozyme: A test of the GROMOS 96 force field against nuclear magnetic resonance data. *Proteins* **2000**, *40*, 145–153.
- (54) Radkiewicz, J. L.; Brooks, C. L., III. Protein dynamics in enzymatic catalysis: Exploration of dihydrofolate reductase. *J. Am. Chem. Soc.* **2000**, *122*, 225–231.
- (55) Pfeiffer, S.; Fushman, D.; Cowburn, D. Simulated and NMR-derived backbone dynamics of a protein with significant flexibility: A comparison of spectral densities for the  $\beta$ -ARK1 PH domain. *J. Am. Chem. Soc.* **2001**, *123*, 3021–3036.
- (56) Wong, K.-B.; Daggett, V. Barstar has a highly dynamic hydrophobic core: Evidence from molecular dynamics simulations and nuclear magnetic resonance relaxation data. *Biochemistry* **1998**, *37*, 11182–11192.
- (57) Brüschweiler, R.; Case, D. A. A collective NMR relaxation model applied to protein dynamics. *Phys. Rev. Lett.* **1994**, *72*, 940–943.
- (58) Lienin, S. F.; Brüschweiler, R. Characterization of collective and anisotropic reorientational protein dynamics. *Phys. Rev. Lett.* **2000**, *84*, 5439–5442.